Available online at www.sciencedirect.com
ScienceDirect
Ceramics International 34 (2008) 1387–1391
CERAMICS INTERNATIONAL
www.elsevier.com/locate/ceramint

Synthesis and characterization of $LiMn_2O_4$/Ag composite by citrate gel and combustion method

Xian Ming Wu *, Shang Chen, Ze Qiang He, Zhuo Bing Xiao, Ming You Ma, Jian Ben Liu

College of Chemistry and Chemical Engineering, Jishou University, Jishou Hunan 416000, China

Received 7 September 2006; received in revised form 9 February 2007; accepted 24 March 2007
Available online 5 May 2007

Abstract

The powder of $LiMn_2O_4$/Ag composite was prepared by citrate gel and combustion technique using lithium acetate, manganese acetate and silver nitrate as starting materials. Phase identification, surface morphology and electrochemical properties were studied by X-ray diffraction, scanning electron microscopy, galvanostatic charge–discharge experiments, and electrochemical impedance spectroscopy. The results show that the powder is the composite of $LiMn_2O_4$ and Ag metal, and silver disperses homogeneously in $LiMn_2O_4$ particles. Compared with $LiMn_2O_4$, $LiMn_2O_4$/Ag composite has higher specific capacity, higher columbic efficiency and lower polarization. The additive of Ag improves the cycleability of $LiMn_2O_4$ powders, especially at higher charge–discharge rate.

Keywords: A. Calcination; B. Composite; C. Impedance; E. Batteries

1. Introduction

Lithium ion or 'rocking-chair' batteries are the state of art of the advanced batteries due to its high potential, high energy density, safety and long shelf life [1–4]. For this battery, conductive fillers are routinely added to the electrodes to construct conductive network, which is essential to compensate for the low electronic conductivity of electrode active materials and to achieve full electrode utilization. The conduction network also enhances battery power and enables faster charge and discharge [2,5]. However, the dispersion of conductive filler in the electrode active materials is not homogeneous for the mixture usually results from the mixing of the two powders.

Researches [6–8] show that synthesis route, synthesis conditions and the different starting materials can greatly affect the characteristics of product. Therefore, to prepare materials with excellent performance, it is important to design and set reasonable synthesis route and conditions.

Citric acid is often used to synthesize composite oxides [6,9,10]. Its multi-functional group can chelate various kinds of cations and react with glycol to form polyester. The pre-ignition of the precursor gel in the open air can facilitate the crystallization and keep suitably partial pressure of oxygen during the calcination at high temperature, which can lead to $LiMn_2O_4$ powders with stable structure and better electrochemical performance. Based on the above-mentioned consideration, we prepared $LiMn_2O_4$/Ag composite by citrate gel and combustion technique and studied its properties as cathode materials for lithium ion batteries.

2. Experimental

Stoichiometric amount of lithium acetate and manganese acetate were dissolved in deionized water. Then citric acid (the molar ratio of the total amount of metal atoms to citric acid is 1:1) and glycol (the molar ratio of glycol to citric acid is 3:2) were added in sequence. After silver nitrate was added into the solution, the mixture was kept under ultrasonic vibration for 15 min followed by a drying at 140 °C for 10 h. The dried precursor gel was ignited in the open air followed by a calcination at 750 °C for 8 h to obtain $LiMn_2O_4$ powders with 5 wt% of silver.

Thermal decomposition behavior of the dried precursor gel was examined by thermogravimetric analysis (TGA) and differential thermal analysis (DTA) at the heating rate of 10 °C min^{-1}. Phase identification and surface morphology of

* Corresponding author.
E-mail address: xianmingwu@163.com (X.M. Wu).

0272-8842/$34.00
doi:10.1016/j.ceramint.2007.03.024

the prepared powders were studied by X-ray diffractometer and scanning electron microscopy.

Electrochemical measurements were conducted through a coin type cell (CR2025) with lithium metal as both counter and reference electrodes, 1 mol L^{-1} $LiPF_6$/EC(ethylene carbonate)–DMC(dimethyl carbonate) solution as electrolyte. Composite cathodes were fabricated as follows: $LiMn_2O_4$/Ag composite, carbon black and polyvinylidene fluoride (PVDF) in the molar ratio of 89.5:3.5:7 were mixed in *n*-methyl pyrrolidinone followed by a vacuum drying at 120 °C for 12 h. The entire cell was assembled in an argon-filled glove box. Galvanostatic charge–discharge experiments were conducted between 4.4 V and 3.3 V, and electrochemical impedance spectroscopy was carried out in the frequency range of 0.02 Hz to 100 kHz with 10 mV amplitude of ac potential.

3. Results and discussion

Fig. 1 shows the thermogravimetric curves of $LiMn_2O_4$/Ag composite precursor gel. The weight loss below 150 °C is caused by the volatilization of the absorbed water and other organic substances, which corresponds to several endothermic peaks in the DTA curves. The weight loss beyond the temperature of 200 °C is associated with the decomposition and combustion of lithium acetate, manganese acetate and other substances, which corresponds to several exothermic peaks in the DTA curves. The weight loss terminates at about 450 °C, indicating that the relevant substances are completely decomposed at this temperature.

The infrared patterns of $LiMn_2O_4$ and $LiMn_2O_4$/Ag composite are displayed in Fig. 2. Two peaks at the wavenumber of 516 cm^{-1} and 623 cm^{-1} are observed in the two figures, which belong to the vibration of Mn–O. There are no obvious differences between the two powders, suggesting that the chemical bonds of the two powders are the same. This indicates that Mn–O bond is not affected by the calcination with Ag.

The X-ray diffraction patterns of $LiMn_2O_4$ and $LiMn_2O_4$/Ag composite are shown in Fig. 3. As seen in the figure, no impurity peaks can be seen except the characteristic patterns of $LiMn_2O_4$, indicating that no new compounds exist in $LiMn_2O_4$/Ag composite, i.e., the $LiMn_2O_4$/Ag system is just a composite of $LiMn_2O_4$ and Ag metal. The crystal parameters of $LiMn_2O_4$ and $LiMn_2O_4$/Ag composite are 8.242 Å and 8.245 Å, respectively. The close parameters of the two powders indicate that silver does not enter the crystal lattice of $LiMn_2O_4$. The figure also shows that no Ag peaks can be observed, which is caused by that the amount of silver additive is too little to be detected.

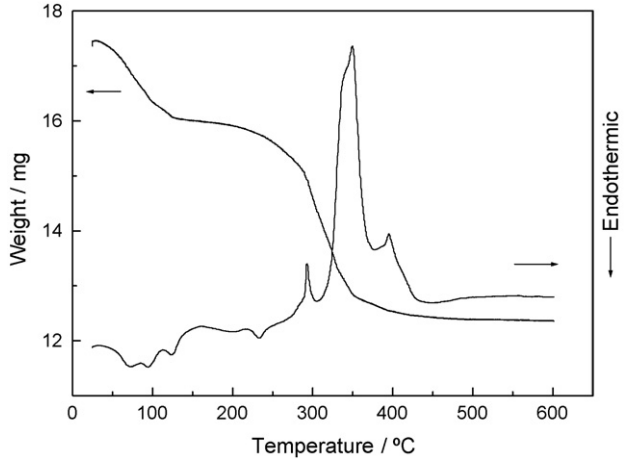

Fig. 1. Thermogravimetric curves of $LiMn_2O_4$/Ag composite precursor gel.

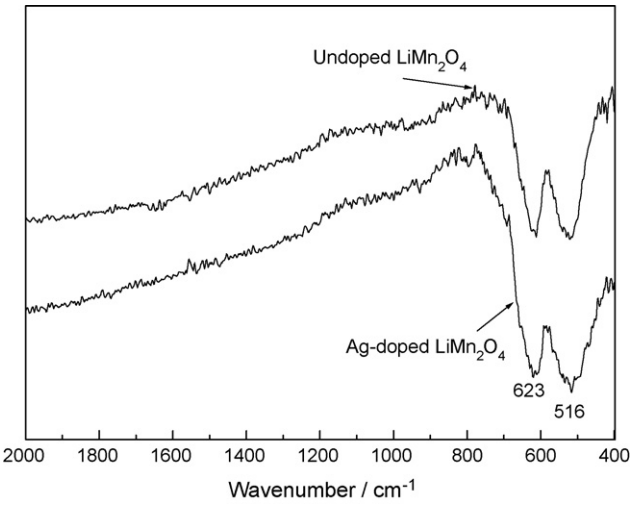

Fig. 2. Infrared patterns of $LiMn_2O_4$ and $LiMn_2O_4$/Ag composite.

The scanning electron micrographs of $LiMn_2O_4$ and $LiMn_2O_4$/Ag composite are presented in Fig. 4. As displayed in the micrograph, there are no obvious differences between the two powders. No silver agglomeration can be observed in $LiMn_2O_4$/Ag composite, which indicates that silver disperses in $LiMn_2O_4$ particles homogeneously. The composite has a narrow particle size distribution of about 1 μm. The small, uniform and narrow particle size distribution of the composite are favorable for the electrochemical properties of high rate capability [11–13].

Fig. 5 displays the charge–discharge curves of $LiMn_2O_4$ and $LiMn_2O_4$/Ag composite at the charge–discharge rate of 0.2 C.

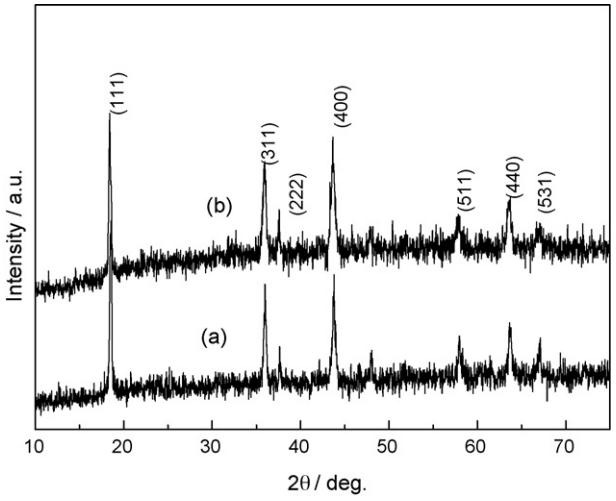

Fig. 3. X-ray diffraction patterns: (a) $LiMn_2O_4$ powder; (b) $LiMn_2O_4$/Ag composite.

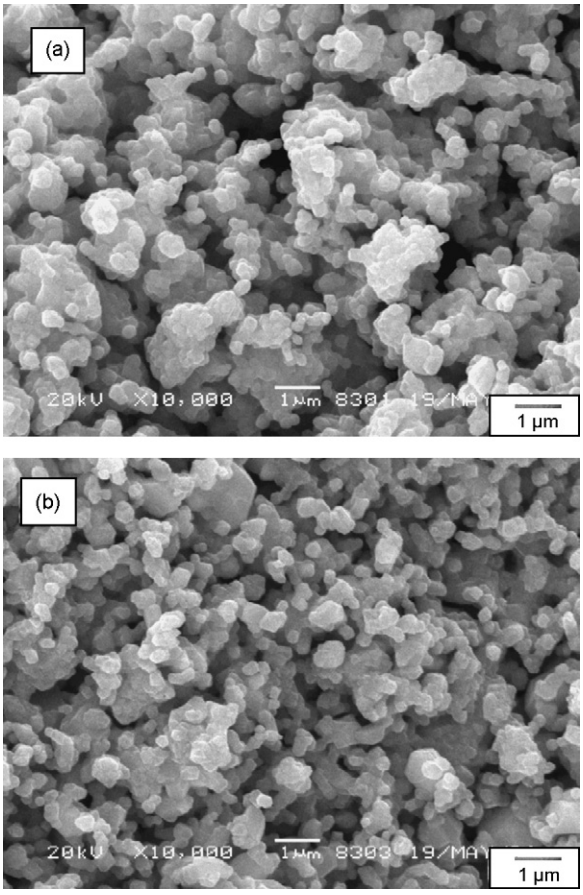

Fig. 4. Scanning electron micrographs: (a) $LiMn_2O_4$ powder; (b) $LiMn_2O_4$/Ag composite.

As observed in the figure, both charge and discharge curves show two clear voltage plateaus, which is the characteristics of $LiMn_2O_4$, suggesting that both the intercalation and deintercalation of lithium-ion are carried out in two steps, which can be written as the following two reversible reactions:

$$\frac{1}{2}Li^+ + \frac{1}{2}e + 2\gamma - MnO_2 \underset{\text{charge}}{\overset{\text{discharge}}{\rightleftharpoons}} Li_{0.5}Mn_2O_4$$

$$\frac{1}{2}Li^+ + \frac{1}{2}e + Li_{0.5}Mn_2O_4 \underset{\text{charge}}{\overset{\text{discharge}}{\rightleftharpoons}} LiMn_2O_4$$

The figure also shows that the discharge voltage plateau and specific capacity of $LiMn_2O_4$/Ag composite are a bit higher than $LiMn_2O_4$. This is caused by the enhanced conductivity due to the doping of silver, which leads to lower ohmic voltage drop and lower overpotential. Calculation shows that the columbic efficiency of $LiMn_2O_4$/Ag composite is about 97%, which is higher than that of 94% for $LiMn_2O_4$ powders.

Fig. 6 presents the electrochemical impedance spectroscopy and its equivalent circuit of $LiMn_2O_4$ and $LiMn_2O_4$/Ag composite. The measurements are performed at the open circuit voltage of 4.03 V after preliminary potentiostatic polarization at the same potential for over 1 h to achieve an equilibrium. The figure shows that the impedance spectroscopy is composed of two semicircles in the high and medium frequency zone, and a line inclined at an angle of 45° to the real axis in the low

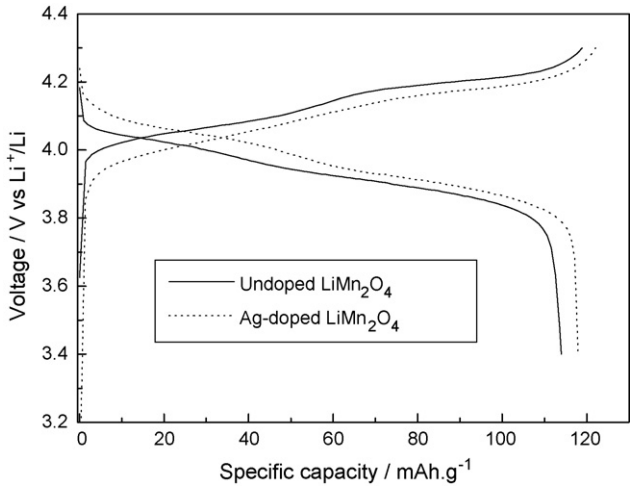

Fig. 5. Charge–discharge curves of $LiMn_2O_4$ and $LiMn_2O_4$/Ag composite.

frequency range. The semicircle in the high frequency range is caused by the formation of solid electrolyte interphase film (SEI film). The medium frequency semicircle is associated with the 'charge transfer reactions' at the interface of the SEI film and oxide electrode, which corresponds to the charge-transfer resistance. The inclined line in the low frequency range is attributable to 'Warburg impedance' that is associated with lithium diffusion through the oxide electrode. In the equivalent circuit, R_e is the electrolyte resistance, R_s the surface film resistance, R_{ct} the charge-transfer resistance, C_s the surface film capacitance, C_d the double layer capacitance, and Z_w the Warburg impedance. From the electrochemical impedance spectroscopy and the equation of $\omega RC = 1$, the values of R_e, R_s, R_{ct}, C_s, and C_d are determined in Table 1. It is noticed that the charge-transfer resistance of $LiMn_2O_4$/Ag composite is smaller than $LiMn_2O_4$. The relatively small charge-transfer resistance of $LiMn_2O_4$/Ag composite is caused by the decrease of the electronic resistivity due to the additive of silver.

The plot of the discharge specific capacity of $LiMn_2O_4$ and $LiMn_2O_4$/Ag composite as a function of discharge rate is shown

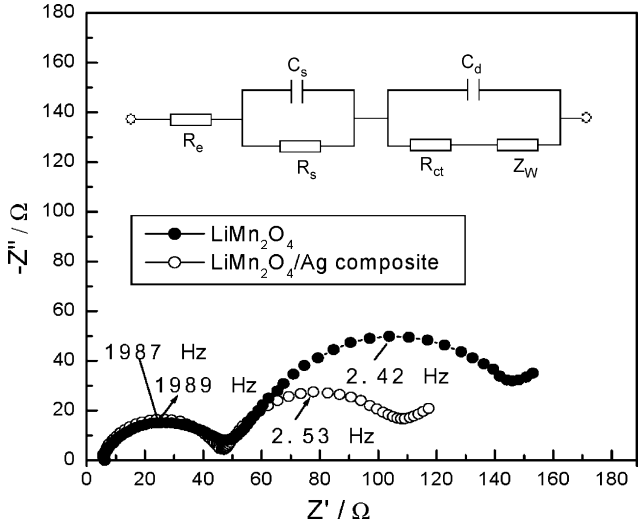

Fig. 6. Complex impedance plots of $LiMn_2O_4$ and $LiMn_2O_4$/Ag composite.

Table 1
Values of R_e, R_s, R_{ct}, C_s, and C_d of $LiMn_2O_4$ and $LiMn_2O_4$/Ag composite

Powders	R_e (Ω)	C_s (F)	R_s (Ω)	C_d (F)	R_{ct} (Ω)
$LiMn_2O_4$	10	0.21×10^{-5}	38	66.52×10^{-5}	98
$LiMn_2O_4$/Ag composite	10	0.22×10^{-5}	36	101.92×10^{-5}	62

in Fig. 7. As seen in the figure, the capacity decreases with the increase of discharge rate. However, the reduction of capacity magnitude for $LiMn_2O_4$/Ag composite is smaller than $LiMn_2O_4$. This suggests that the additive of silver can help keep higher specific capacity, especially at higher discharge rate.

The cycling behaviors of $LiMn_2O_4$ and $LiMn_2O_4$/Ag composite cycling at different charge–discharge rates are displayed in Fig. 8. The cycle number of the measurement is 20. As observed in the figure, when the charge–discharge rate is 0.2 C, the capacity retention of $LiMn_2O_4$/Ag composite is slightly lower than $LiMn_2O_4$. However, the capacity retention of $LiMn_2O_4$/Ag composite becomes higher than $LiMn_2O_4$ when the charge–discharge rate reaches 0.4 C, and gets much higher than $LiMn_2O_4$ with further increase of charge–discharge rate, which indicates that Ag additive is significantly beneficial to the improvement of the reversible capacity and cycling stability, especially at higher charge–discharge rate.

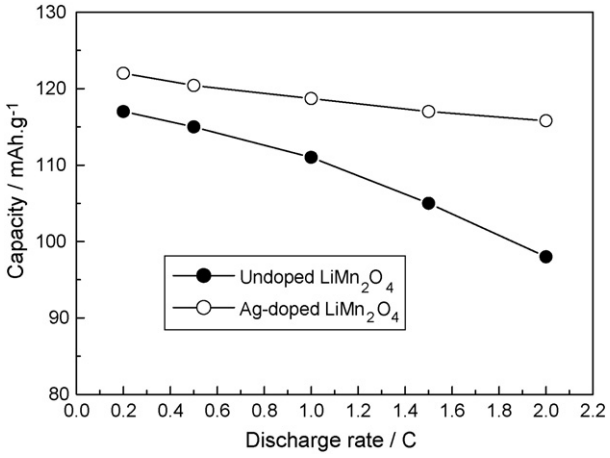

Fig. 7. Specific capacity of $LiMn_2O_4$ and $LiMn_2O_4$/Ag composite discharging at different rates.

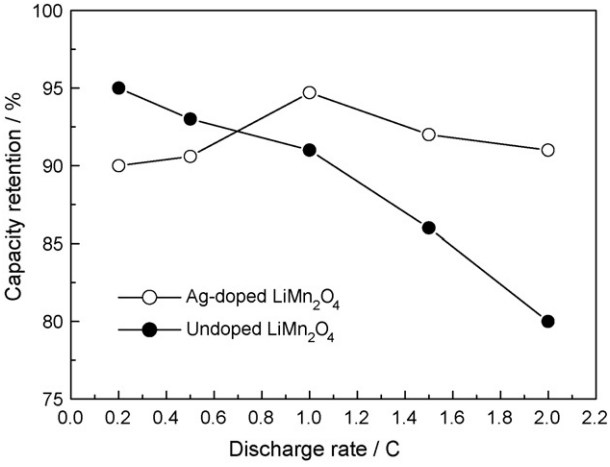

Fig. 8. The cycling behaviors of $LiMn_2O_4$ and $LiMn_2O_4$/Ag composite after being cycled 20 times at different charge–discharge rates.

4. Conclusions

$LiMn_2O_4$/Ag composite prepared by citrate gel and combustion method is the composite of $LiMn_2O_4$ and Ag metal. The composite has a small, uniform and narrow particle size distribution. The $LiMn_2O_4$/Ag composite has a higher specific capacity, higher columbic efficiency, and lower polarization than $LiMn_2O_4$. The charge-transfer resistance of $LiMn_2O_4$/Ag composite is smaller than $LiMn_2O_4$. During the cycling, the capacity retention of $LiMn_2O_4$/Ag composite is slightly lower than $LiMn_2O_4$ at low charge–discharge rate. However, the capacity retention becomes higher than $LiMn_2O_4$ with the increase of charge–discharge rate. Ag additive is significantly beneficial to the improvement of cycling stability for $LiMn_2O_4$ powders, especially at higher charge–discharge rate.

Acknowledgment

This work was supported by Hunan Provincial Natural Science Foundation of China (No. 04JJ40038).

References

[1] P. Arora, R.E. White, M. Doyle, Capacity fade mechanisms and side reactions in lithium-ion batteries, J. Electrochem. Soc. 145 (1998) 3647–3667.
[2] D. Guyomard, J.M. Tarascon, The carbon/$Li_{1+x}Mn_2O_4$ system, Solid State Ionics 69 (1994) 222–237.
[3] M.N. Richard, E.W. Fuller, J.R. Dahn, The effect of ammonia reduction on the spinel electrode materials, $LiMn_2O_4$ and $Li(Li_{1/3}Mn_{5/3})O_4$, Solid State Ionics 73 (1994) 81–91.
[4] D. Guyomard, J.M. Tarascon, Synthesis conditions and oxygen stoichiometry effects on Li insertion into the spinel $LiMn_2O_4$, J. Electrochem. Soc. 141 (1994) 1421–1431.
[5] Z.X. Shu, R.S. McMillan, J.J. Murray, Electrochemical intercalation of lithium into graphite, J. Electrochem. Soc. 140 (1993) 922–927.
[6] B.J. Hwang, R. Santhanam, D.G. Liu, Effect of various synthetic parameters on purity of $LiMn_2O_4$ spinel synthesized by a sol–gel method at low temperature, J. Power Sources 101 (2001) 86–89.
[7] H. Gadjov, M. Gorova, V. Kotzeva, G. Avdeev, S. Uzunova, D. Kovacheva, $LiMn_2O_4$ prepared by different methods at identical thermal treatment conditions: structural, morphological and electrochemical characteristics, J. Power Sources 134 (2004) 110–117.
[8] S.S. Zhang, T.R. Jow, Optimization of synthesis condition and electrode fabrication for spinel $LiMn_2O_4$ cathode, J. Power Sources 109 (2002) 172–177.

[9] D.W. Kim, S.G. Oh, Agglomeration behavior of chromia nanoparticles prepared by amorphous complex method using chelating effect of citric acid, Mater. Lett. 59 (2005) 976–980.
[10] R. Pasricha, V. Ravi, Synthesis of $Sr_{0.5}Ba_{0.5}Nb_2O_6$ by citrate gel method, Mater. Chem. Phys. 94 (2005) 34–36.
[11] C.J. Patrissi, C.R. Martin, Sol–gel-based template synthesis and Li-insertion rate performance of nanostructured vanadium pentoxide, J. Electrochem. Soc. 146 (1999) 3176–3180.
[12] H.L. Chen, X.P. Qiu, W.T. Zhu, P. Hagenmuller, Synthesis and high rate properties of nanoparticled lithium cobalt oxides as the cathode material for lithium-ion battery, Electrochem. Commun. 4 (2002) 488–491.
[13] N. Li, C.J. Patrissi, G. Che, C.R. Martin, Rate capabilities of nanostructured $LiMn_2O_4$ electrodes in aqueous electrolyte, J. Electrochem. Soc. 147 (2000) 2044–2049.